

Diazotization of the Amino Acid [*closo*-1-CB₉H₈-1-COOH-6-NH₃] and Reactivity of the [*closo*-1-CB₉H₈-1-COO-6-N₂][−] Anion

Bryan Ringstrand,^{†,‡} Piotr Kaszynski,^{*,†,§} and Victor G. Young, Jr.^{‡,¶}

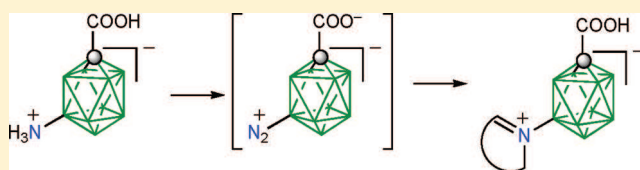
[†]Organic Materials Research Group, Department of Chemistry, Vanderbilt University, Nashville, Tennessee 37235, United States

[§]Faculty of Chemistry, University of Lodz, Tamka 12, 91403 Lodz, Poland

[‡]Crystallographic Laboratory, Department of Chemistry, University of Minnesota, Twin Cities, Minnesota 55455, United States

S Supporting Information

ABSTRACT: A comparative study of the reactivity of dinitrogen acids [*closo*-1-CB₉H₈-1-COOH-10-N₂] (3[10]) and [*closo*-1-CB₉H₈-1-COOH-6-N₂] (3[6]) was conducted by diazotization of a mixture of amino acids [*closo*-1-CB₉H₈-1-COOH-6-NH₃] (1[6]) and [*closo*-1-CB₉H₈-1-COOH-10-NH₃] (1[10]) with NO⁺BF₄[−] in the presence of a heterocyclic base (pyridine, 4-methoxypyridine, 2-picoline, or quinoline). The 10-amino acid 1[10] formed an isolable stable 10-dinitrogen acid 3[10], while the 6-dinitrogen carboxylate 3[6][−] reacted in situ, giving products of N-substitution at the B6 position with the heterocyclic solvent (4[6]). The molecular and crystal structures for pyridinium acid 4[6]a were determined by X-ray crystallography. The electronic structures and reactivity of the 6-dinitrogen derivatives of the {1-CB₉} cluster were assessed computationally at the B3LYP/6-31G(d,p) and MP2/6-31G(d,p) levels of theory and compared to those of the 10-dinitrogen, 2-dinitrogen, and 1-dinitrogen analogues.



INTRODUCTION

Apical dinitrogen derivatives of the [*closo*-B₁₀H₁₀]^{2−} and [*closo*-1-CB₉H₁₀][−] clusters have been shown to be isolable and stable^{1–8} intermediates used in the preparation of a variety of nitrogen,^{1–6,8} sulfur,^{3,5,6,9–11} oxygen,^{3,12} and even carbon³ derivatives, which include liquid crystals.^{10,13–16} The robustness of such dinitrogen derivatives originates from the electronic interaction between the cluster and the N₂ group, which appears to be general for the apical positions (positions 1 and 10) of the 10-vertex *closo*-boranes.¹⁷ However, to the best of our knowledge, derivatives of 10-vertex *closo*-boranes with the dinitrogen group at the equatorial position have not been investigated either experimentally or computationally. One obstacle to experimental studies of such derivatives of the {1-CB₉} cluster is the lack of appropriate amino derivatives.

Recently, we demonstrated⁶ the preparation of amino acid [*closo*-1-CB₉H₈-1-COOH-10-NH₃] (1[10]) by palladium-catalyzed amination of iodo acid [*closo*-1-CB₉H₈-1-COOH-10-I] (2[10]), which was separated from isomeric iodo acid 2[6].¹⁸ Our preliminary results indicated that the amination procedure is effective for a mixture of iodo acids 2[10] and 2[6], and a mixture of amino acids [*closo*-1-CB₉H₈-1-COOH-6-NH₃] (1[6]) and 1[10] could be obtained.⁶ Diazotization of this mixture of amino acids would provide an opportunity to study the generation and reactivity of [*closo*-1-CB₉H₈-1-COOH-6-N₂] (3[6]), the first example of an equatorial dinitrogen derivative of a 10-vertex *closo*-borane.

Here, we report comparative studies of diazotization reactions of a mixture of amino acids 1[6] and 1[10] in solutions of heteroaromatic bases (pyridine, *p*-methoxypyridine, 2-picoline,

and quinoline), the formation of dinitrogen acids 3[6] and 3[10], and their reactivity. The heterocycles were chosen in such a way as to vary their basicity and steric effects. The structure of one of the reaction products was confirmed by single-crystal X-ray analysis. The experimental results are augmented with computational analysis of the electronic structures and thermodynamic stability of selected B6 derivatives and a comparison to their isomeric B10, B2, and C1 analogues.

RESULTS AND DISCUSSION

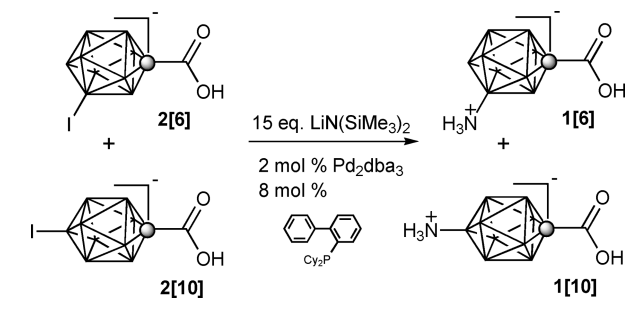
Synthesis. A 4:1 mixture of iodo acids 2[6] and 2[10] was aminated with LiN(SiMe₃)₂ in the presence of Pd(0) using conditions previously described for the pure 2[10] derivative (Scheme 1).⁶ The amino acids 1[6] and 1[10] were obtained in about a 5:1 ratio and 37% yield. In another experiment, the ratio of isolated amino acids increased to 12:1 with a yield of 47%.¹⁹ The mixture was contaminated with up to 7% of the parent acid [*closo*-1-CB₉H₈-1-COOH][−] and used in subsequent studies without further separation.

We previously demonstrated that, for successful diazotization of 1[10] and the formation of dinitrogen acid 3[10], the reaction mixture must contain a base such as pyridine.⁶ Diazotization of a mixture of amino acids under these conditions (MeCN containing pyridine) gave 3[10], the 6-pyridinium derivative [*closo*-1-CB₉H₈-1-COOH-6-C₅H₅N] (4[6]a), and another {1-CB₉} product derived presumably from MeCN. To eliminate side

Received: December 22, 2010

Published: February 22, 2011

Scheme 1



reactions with MeCN, diazotization reactions were conducted in neat pyridine. A reaction of enriched 6-amino acid **1[6]** (~90% pure) with NO^+BF_4^- in pyridine at -20°C gave 6-pyridinium acid **4[6]****a** as the sole product isolated in 58% yield (entry 1, Table 1), with only traces of 10-dinitrogen acid **3[10]** observed by ^{11}B NMR (Scheme 2). As in experiments with pure 10-amino acid **1[10]**, no 10-pyridinium acid **4[10]****a** was detected under these conditions.

A similar reaction of a 5:1 mixture of the amino acids in neat 4-methoxypyridine gave full conversion of the reactants to 6-onium acid **4[6]****b** and 10-dinitrogen acid **3[10]** as the only products observed in ^{11}B NMR. The former was isolated by chromatography in 73% yield corrected for the content of **1[6]** in the starting mixture (entry 2, Table 1). Diazotization reactions in 2-picoline (entry 3, Table 1) and quinoline (entry 4, Table 1) gave incomplete transformations of the amino acids. The 6-onium acids, **4[6]****c** and **4[6]****d**, were the only products observed by ^{11}B NMR and isolated in 24% and 3% yield, respectively, after chromatographic separation. The absence of 10-dinitrogen acid **3[10]** in the reaction mixtures indicates that 10-amino acid **1[10]** was unreactive in these two solvents. The incompleteness of the reactions with quinoline could be due to its lower basicity than that for pyridine ($\text{p}K_{\text{a}} = 5.23$ for pyridinium,²⁰ 6.47 for 4-methoxypyridinium,²¹ 5.96 for 2-picolinium,²⁰ and 4.94 for quinolinium²²), although increased steric demand of quinoline relative to that of pyridine cannot be excluded. Poor results for diazotization in 2-picoline are most likely due to the presence of the methyl group, which hinders the NO^+ transfer or promotes side reactions.

Attempts to introduce other fragments at the 6 position of amino acid **1[6]** such as butoxy (conditions: butyl nitrite, butanol, Hünig's base, and reflux) and dimethylsulfonium (conditions: Me_2S , Hünig's base, and NO^+BF_4^-) were unsuccessful, and only the starting amino acids were recovered.

Molecular Structure. The structure of **4[6]****a** was confirmed by single-crystal X-ray analysis, and selected bond lengths and angles are shown in Figure 1.²³ Colorless crystals of 6-pyridinium acid **4[6]****a** were grown by the slow evaporation of an aqueous EtOH solution.

Acid **4[6]****a** forms a dimeric structure in the solid state through synergetic hydrogen bonds [$\text{O}\cdots\text{H}\cdots\text{O}$: $d_{\text{OO}} = 2.6288(14)$ Å; $\alpha_{\text{OHO}} = 175.7^\circ$]. The carboxyl group in the acid adopts a nearly eclipsed conformation relative to the $\{\text{closo-1-CB}_9\}$ cage with a dihedral angle of about 6.6° , which significantly deviates from the staggered conformation found computationally in **4[6]****a** and observed⁶ experimentally in 10-pyridinium acid **4[10]****a**. The pyridine ring in the solid-state structure of **4[6]****a** adopts a nearly eclipsed orientation relative to the B6–B10 bond with a dihedral

Table 1. Results for Diazotization of Mixtures of **1[6]** and **1[10]**^a

entry	solvent	conversion (%) ^b	yield of 4[10] (%) ^c
1	pyridine	100	a, 58 ^d
2	4-methoxypyridine	100	b, 73 ^d
3	2-picoline	50	c, 24 ^e
4	quinoline	30	d, 3 ^e

^a Reaction conditions: 3 equiv of NO^+BF_4^- added to a solution of 0.5 mmol of **1** in ~3 mL of solvent at -20°C (entries 1–3) or 0°C (entry 4); reaction time 3 h. The ratio of **1[6]**/**1[10]** in entry 1 is 12:1, and that in entries 3 and 4 is 5:1. ^b Percent of reacted amino acid **1[6]** by ^{11}B NMR. ^c After chromatographic separation and calculation based on the content of amino acid **1[6]** in the mixture. ^d Dinitrogen acid **3[10]** was observed in the crude reaction mixture. ^e Dinitrogen acid **3[10]** was not observed in the crude reaction mixture.

angle (C–N–B–B) of $6.09(19)^\circ$. B3LYP/6-31G(d,p) results show that both orientations of the pyridine ring, parallel and perpendicular to the B6–B10 bond, are conformational minima, with the latter favored thermodynamically, according to MP2/6-31G(d,p) calculations. The B–N bond length of 1.5470(18) Å observed in **4[6]****a** is slightly longer than the analogous distance of 1.525(3) Å found in **4[10]****a**.⁶ The unit cell contains two pairs of molecules related by inversion centers.

Mechanistic Analysis. The reaction of 6-amino acid **1[6]** and the formation of pyridinium adduct **4[6]** appear to be similar to that of the 10-amino acid **1[10]** and presumably involve deprotonation of the ammonium group, diazotization of the resulting amino group, and decomposition of the apparently unstable dinitrogen derivative **3[6]**[−]. The resulting boronium ylide **5[6]**[−] is trapped with nucleophilic pyridine (Scheme 3). Formation of the N-regioisomer **4[6]** as the only observable product supports heterolytic cleavage of the B–N bond in **3[6]** and formation of the ylide **5[6]**[−] and is consistent with that of the 10-isomer **3[10]**. In contrast, the C1 dinitrogen derivative [*closo-1-CB₉H₉-1-N₂*] (**6[1]**) undergoes nucleophile-assisted homolytic cleavage of the C–N bond and yields C-substituted pyridine.⁵ For a better understanding of the experimental results for **1[6]** and **1[10]**, we conducted theoretical analyses for a series of four isomeric derivatives of $\{\text{1-CB}_9\}$, which for simplicity were lacking the COOH group.

MP2/6-31G(d,p) level calculations demonstrated that the parent [*closo-1-CB₉H₉-6-NH₂*] is highly basic. Using Scheme 4 and the experimental $\text{p}K_{\text{a}}$ value²⁴ for [*closo-1-CB₁₁H₁₁-1-NH₃*], its $\text{p}K_{\text{a}}$ was estimated at 18.1, which is lower by 3.7 than $\text{p}K_{\text{a}}$ for the 10-amino analogue [*closo-1-CB₉H₉-10-NH₂*] in aqueous EtOH (Table 2). This suggests that the equilibrium in Scheme 3 is shifted further to the right for [*closo-1-CB₉H₈-1-COO-6-NH₃*] (**1[6]**[−]) than for the 10-isomer **1[10]**[−] and the higher concentration of free amine [*closo-1-CB₉H₈-1-COO-6-NH₂*] (**1[6]**^{2−}) in the solution results in faster diazotization of 6-amino than the 10-amino isomer. This is consistent with the experimental results, which show that in quinoline, which is less basic than pyridine, conversion of **1[6]**[−] is much faster than that of its 10-isomer **1[10]**[−]. A comparison of the four isomeric amines [*closo-1-CB₉H₉-NH₂*] demonstrates that the closer the substituent is to the C1 position, the less basic the amine is (Table 2).

The parent 6-dinitrogen derivative [*closo-1-CB₉H₉-6-N₂*] (**6[6]**) is the least stable among the four regioisomers **6**. The calculated free energy $\Delta G_{298} = 18.1$ kcal/mol for heterolysis of the B–N bond in **6[6]** is lower by nearly 13 kcal/mol than that

Scheme 2

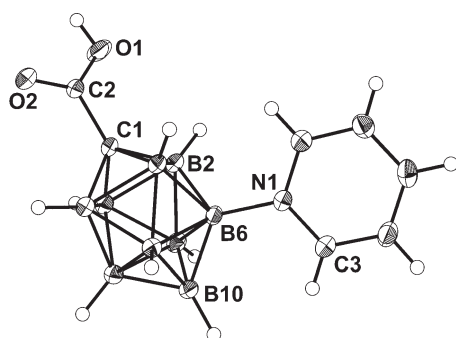
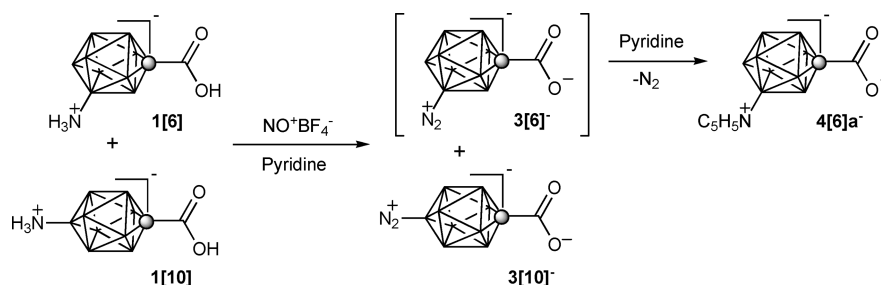
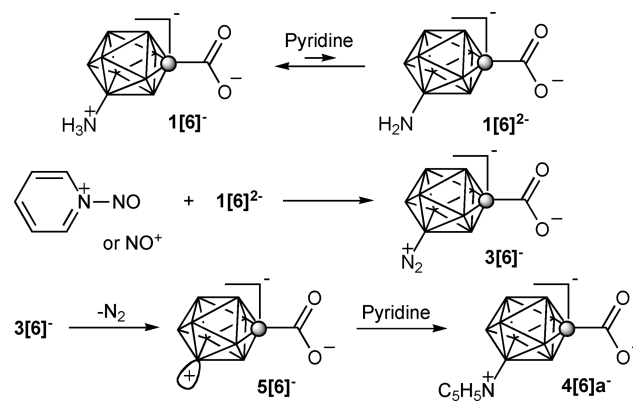


Figure 1. Thermal ellipsoid diagram representations of 4[6]a $^-$ and drawn at 50% probability. Selected interatomic distances (Å) and angles (deg): B6–N1, 1.5470(18); C1–B (av), 1.6089; C1–C2, 1.4835(18); C1 \cdots B10, 3.543; C2–C1–B (av), 125.7; N1–B6–B10, 121.59(11); O1–C2–O2, 123.54(12); C3–N1–B6–B10, 6.09(19); C3–N1–B6–B2, 139.18(12); O1–C2–C1–B2, $-6.6(2)$.

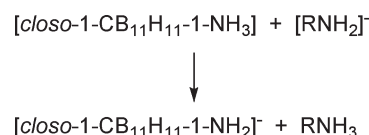
for the 10-dinitrogen isomer 6[10] and by about 5 kcal/mol than those for 6[1] and 6[2].²⁵ The order of stability, 6[10] > 6[1] ~ 6[2] > 6[6], is consistent with experimental observations showing that the dinitrogen acid 3[10] is stable to storage, and in solutions at ambient temperature, 6[1] is stable in the solid state but slowly decomposes in solutions at ambient temperature, while the 3[6] $^-$ derivative easily undergoes dissociation even at low temperatures. Computational results demonstrate that the 2-dinitrogen derivative 6[2] has a stability comparable to that of 6[1], which suggests the possibility of its isolation.

The difference in the stability of the dinitrogen group in 6 originates in the efficiency of the molecular orbital (MO) overlap between the N_2 fragment and the {1-CB₉} cage and also the electron density at the point of attachment to the cage. In the apical isomers 6[10] and 6[1], the double-degenerate π -symmetry MO of the cage provides electronic communication with the N_2 π system, which is more effective than that between the nondegenerate π -symmetry MO of the {1-CB₉} cage and N_2 in the equatorial isomers 6[6] and 6[2] (Figure 2). Analysis of the bonding in the three B isomers shows that the B–N distance increases from 1.459 Å in the 10-isomer 6[10] to 1.491 Å in 6[6] to 1.499 Å in the 2-isomer 6[2] (Table 3). At the same time, the N–N distance decreases from 1.138 to 1.135 Å in the same order. This trend is paralleled by Wiberg bond index (WBI) values, which indicate a progressively weaker B–N bond and increasing triple-bond character between the N atoms in the series 6[10], 6[6], and 6[2] (Table 3). This is consistent with the lower enthalpy of decomposition of the two equatorial dinitrogen derivatives 6[6] and 6[2] than the axial analogue 6[10] by

Scheme 3



Scheme 4



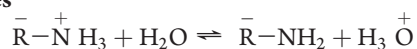
13.1 and 8.0 kcal/mol, respectively. The 2-dinitrogen derivative 6[2] has a higher endotherm of decomposition than is expected from the WBI trend because of the significantly lower electron density of the B2 atom than the B6 atom measured by the atomic charge q_B of +0.13 versus -0.08 (Table 3).

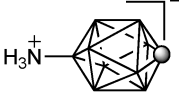
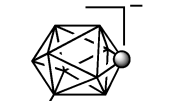
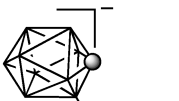
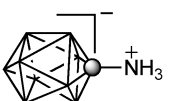
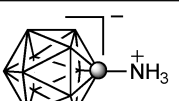
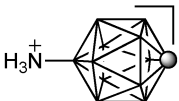
Analysis of the data for 1-dinitrogen 6[1] demonstrates that it has higher bond order between the cage and N_2 fragment and significantly less triple-bond character between the N atoms than was observed in the B isomers (Table 3). It is, however, less thermodynamically stable than might be expected from the trend in WBI because of higher negative atomic charge of the C atom ($q_C = -0.52$) and, consequently, a lower tendency to retain the N_2 fragment.

This analysis is consistent with the results for benzenediazonium ions, in which substituents that increase the electron density at the C1 atom stabilize the transition state and, hence, destabilize the diazonium ion, while electron-withdrawing substituents stabilize the cation against heterolysis.²⁶

Overall, the N_2 fragment is the least strongly held by the {1-CB₉} cage in the 6 position, and the B6–N bond most easily undergoes heterolysis, forming ylide 7[6].

Table 2. Calculated pK_a for Selected Ammonium Derivatives^a



$\bar{R}-\overset{+}{N}H_3$	pK_a^b
	22.8
	18.1
	16.5
	9.1
	6.0 ^c
	21.4

^a MP2/6-31+G(d,p)//MP2/6-31G(d,p) with density functional theory thermodynamic corrections in a 50% aqueous EtOH dielectric medium ($\epsilon = 52.5$). ^b pK_a values were calculated from a change of the free energy ΔG_{298} in a proton-transfer reaction in Scheme 4 and the experimental value for [closo-1-CB₁₁H₁₁-1-NH₃] ($pK_a = 6.0$ in 50% EtOH; ref24). ^c Experimental value.²⁴

A comparison of the electronic structures of the ylides demonstrated that the lowest unoccupied MO (LUMO) of ylide 7[6] has the highest energy ($E_{LUMO} = +0.4$ eV; Figure 3), which results in its lowest electrophilicity among the four structures. This is consistent with the lowest exotherm of reaction with pyridine (-77.1 kcal/mol) compared to other ylides 7.²⁵ The lowest energy of the LUMO is calculated for the C1 isomer 7[1] ($E_{LUMO} = -1.57$ eV), which corresponds to the highest exotherm for reaction with pyridine (-103.5 kcal/mol).

The exotherm of the overall transformation of dinitrogen 6 to pyridine 8 follows the order 6[1] > 6[2] > 6[10] > 6[6], with the 10-isomer 6[10] having a higher exotherm than the 6-isomer 6[6] by about 1.5 kcal/mol.²⁵

A comparison of the calculated enthalpies of formation for isomeric derivatives of {1-CB₉} indicates that the B derivatives are more stable than the C1 analogues by 31–57 kcal/mol (Table 4). Among the B-dinitrogen and B-pyridinium

derivatives, the 10- and 6-isomers have comparable stability, while the B2 analogues are generally less thermodynamically stable. In contrast, the 6-boronium ylide 7[6] appears to be more stable than the 10-isomer 7[10] by 12.1 kcal/mol, according to MP2/6-31G(d,p) level calculations in the gas phase.

The process for transformation of the dinitrogen carboxylate anions 3[−], which exist in pyridine solutions (Figure 4), to pyridinium derivatives is similar to that of the parent dinitrogen compounds 6. Heterolysis of the B–N bond is more favorable for the 6-isomer 3[6][−] than for the 10-isomer 3[10][−] by nearly 14 kcal/mol. The calculated ΔG_{298} of 17.2 kcal/mol for the former is sufficiently low for the process to take place in situ at low temperature, while ΔG_{298} of 31.3 kcal/mol for the 10-isomer 3[10][−] is high enough for the compound to be stable under these conditions.

Electronic Spectroscopy. The UV absorption spectrum of 4[6]a in MeCN showed a moderately strong absorption band with a maximum at 264 nm and vibronic splitting of about 810 cm^{−1} (Figure 5). This is essentially the same wavelength as that recorded⁶ for the 10-vertex pyridinium acid 4[10]a. ZINDO//MP2/6-31G(d,p) level calculations for global minima of 4[10]a and 4[6]a revealed that their lowest energy transitions occur at 351 and 352 nm, respectively, and involves excitation from the highest occupied MO, localized mainly on the cage, to the LUMO, localized on the pyridine ring. Both transitions exhibit a significant hypsochromic shift, and in a MeCN dielectric medium, the transitions are calculated at 303 nm for 4[10]a and 317 nm for 4[6]a.²⁷

Excitation of 4[10]a at 263 nm results in a weak fluorescence with a maximum at 426 nm. No emission was observed for the 6-pyridinium analogue 4[6]a.

SUMMARY AND CONCLUSIONS

The results demonstrate that 6-iodo acid 2[6] can be effectively aminated using LiN(SiMe₃)₂ in the presence of Pd(0). Diazotization of the resulting 6-amino acid 1[6] in solutions of aromatic amines leads to the replacement of the NH₂ group with a solvent molecule. The mechanism involves the initial formation of the unstable 6-dinitrogen derivative 3[6], which in situ undergoes heterolysis of the B–N bond. The resulting electrophilic boronium ylide 5[6][−] is trapped by a nucleophilic solvent. The reaction appears to be efficient and synthetically useful for basic and sterically unhindered heteroaromatic bases such as pyridine and 4-methoxypyridine.

The results of theoretical analysis of the two dinitrogen carboxylate anions 3[6][−] and 3[10][−] and a series of regioisomeric amino and dinitrogen derivatives of {closo-1-CB₉} are consistent with experimental data. Analysis of a series of isomeric amines demonstrates that their basicity increases with an increase in the distance from the C1 position. A comparison of the electronic structures and stabilities of the parent dinitrogen derivatives 6 shows significant differences between C–N and B–N bonding in the series and the importance of the electron density at the substitution site for their stability. Computational results suggest that the stability of the dinitrogen derivatives can be increased by using electron-withdrawing substituents on the cage, which decrease the electron density of the atom substituted with the N₂ fragment.

The presented findings open up the possibility for conversion of other B-amino compounds, whose pK_a is not greater than that of 1[10], to pyridinium derivatives. Computational results

indicate that amino derivatives of the {*closo*-1-CB₁₁} cluster are suitable substrates for such a diazotization/substitution reaction, while amino derivatives of {*closo*-B₁₂} and {*closo*-B₁₀} clusters are too basic for the process to be efficient.²⁸ The introduction of other

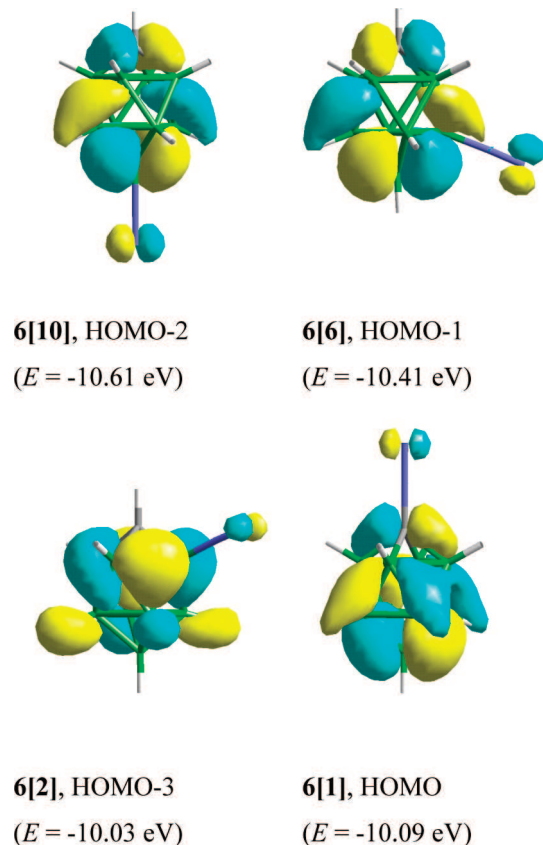


Figure 2. MP2/6-31G(d,p)-derived contours and energies for the relevant MOs of dinitrogen derivatives **6**. For **6[10]** and **6[1]**, only one of the two degenerate MOs is shown.

Table 3. Bonding Properties of the Isomeric Dinitrogen Derivatives^a

	6[10]	6[6]	6[2]	6[1]
$d_{X-N}/\text{\AA}$	1.459	1.491	1.499	1.337
$d_{N-N}/\text{\AA}$	1.138	1.136	1.135	1.149
WBI_{X-N}	0.80	0.76	0.74	1.03
WBI_{N-N}	2.47	2.50	2.51	2.33
X	$\text{sp}^{6.0}$	$\text{sp}^{6.0}$	$\text{sp}^{5.2}$	$\text{sp}^{3.4}$
N	$\text{sp}^{0.65}$	$\text{sp}^{0.65}$	$\text{sp}^{0.66}$	$\text{sp}^{0.8}$
q_X	-0.13	-0.08	+0.13	-0.52
q_N	+0.14	+0.13	+0.13	+0.21

^a NBO analysis of the MP2/6-31G(d,p) wave function. X = B for **6[10]**, **6[6]**, and **6[2]**. X = C for **6[1]**.

substituents using this diazotization method still poses a challenge because of the solubility of the amino acid and compatibility of the solvent/nucleophile with the nitronium cation.

COMPUTATIONAL DETAILS

Quantum mechanical calculations were carried out with the B3LYP^{29,30} and MP2(fc)³¹ methods with a 6-31G(d,p) basis set using the *Gaussian 09* package.³² Geometry optimizations were undertaken using the appropriate symmetry constraints and tight convergence limits. Vibrational frequencies were used to characterize the nature of the stationary points and to obtain thermodynamic parameters. Zero-point-energy corrections were scaled by 0.9806.³³ Hybridization parameters, WBI matrices, and natural charges were obtained using the natural bond order (NBO) algorithm supplied in the *Gaussian 09* package.³² Population analysis of the MP2 wave function (MP2//MP2) was performed using the DENSITY(MP2) keyword. The isodensity polarizable continuum solvation model (IPCM)³⁴ was used with default parameters and $\epsilon = 52.5$ for EtOH/H₂O (1:1, v/v) at 25 °C, which was interpolated from the reported values for EtOH/H₂O mixtures.³⁵

Table 4. Relative Thermodynamic Stability for Selected Pairs of Isomers^a

X	$\Delta H = H_{[1]} - H_{[10]}$ (kcal/mol)	$\Delta H = H_{[1]} - H_{[6]}$ (kcal/mol)	$\Delta H = H_{[1]} - H_{[2]}$ (kcal/mol)
N ₂	+52.4	+50.4	+38.4
+ ^b	+44.5	+56.6	+41.9
pyridinium	+38.9	+38.1	+31.0

^a The MP2/6-31G(d,p) level with density functional theory thermodynamic corrections. The difference in the enthalpy of formation between the [1] and [X] isomers. ^b Vacant orbital in the glide.

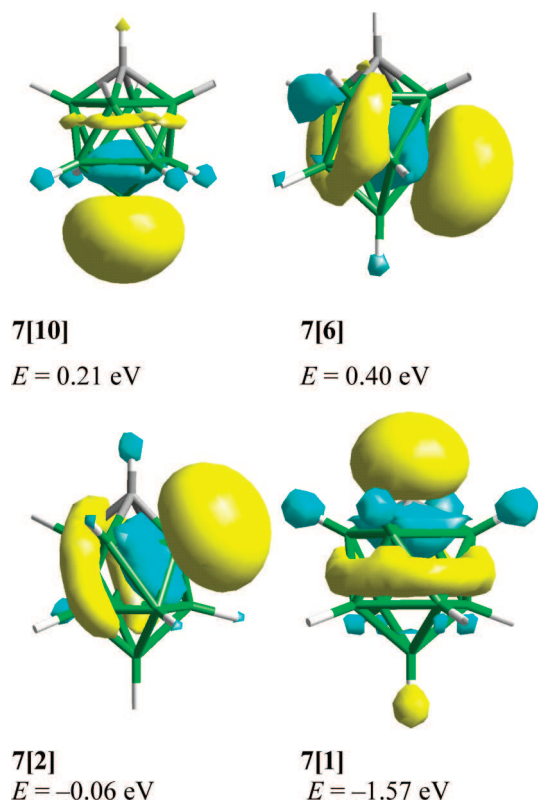


Figure 3. MP2/6-31G(d,p)-derived contours and energies for the LUMO of ylides 7.

Excitation energies for 6-pyridinium acid 4[6]a were obtained at its MP2-determined geometry using the INDO/2 algorithm (ZINDO)³⁶ as supplied in Cerius2 suite of programs and including all electrons and orbitals in the configuration interaction. ZINDO calculations with the solvation model (self-consistent reaction field, SCRF) in the MeCN medium ($\epsilon = 36.64$, $n = 1.3441$) used cavity radii (5.02 Å for 4[10]a and 5.10 Å for 4[6]a) derived from the MP2 calculations with the VOLUME and DENSITY(MP2) keywords.

EXPERIMENTAL SECTION

Reagents and solvents were obtained commercially. Pyridine, 4-methoxy-pyridine, 2-picoline, and quinoline were distilled from CaH_2 , stored over KOH, and distilled from KOH when needed. All other reagents were used as supplied. Reactions were carried out under argon, and subsequent manipulations were conducted in air. NMR spectra were obtained at 128.4 MHz (^{11}B) and 400.1 MHz (^1H) in CD_3CN unless otherwise specified. ^1H NMR spectra were referenced to the solvent and ^{11}B NMR chemical shifts to an external boric acid sample in CH_3OH , which was set to 18.1 ppm. Ultraviolet absorption spectra were recorded in Optima-grade CH_3CN .

General Procedure for Diazotization of a Mixture of Amino Acids 1[6] and 1[10]. Under argon, a mixture of amino acids 1[6] and 1[10] (0.5 mmol) was dissolved in neat amine (~3 mL) and cooled to -20°C (reactions in quinoline were run at 0°C). To the resulting light-yellow solution was added NO^+BF_4^- (3 equiv), and the reaction mixture was stirred for 3 h at the same temperature. The reaction mixture was diluted with 10% HCl (30 mL), and the products were extracted into Et_2O ($3 \times 10 \text{ mL}$). The combined Et_2O layers were washed with 10% HCl (30 mL) and dried (Na_2SO_4), and the solvents were evaporated to dryness. The crude product was passed through a short silica gel plug ($\text{CH}_3\text{OH}/\text{CH}_2\text{Cl}_2$, 1:19) and washed with boiling isooctane followed by hot water, and analytical samples of 4[6]a–4[6]c

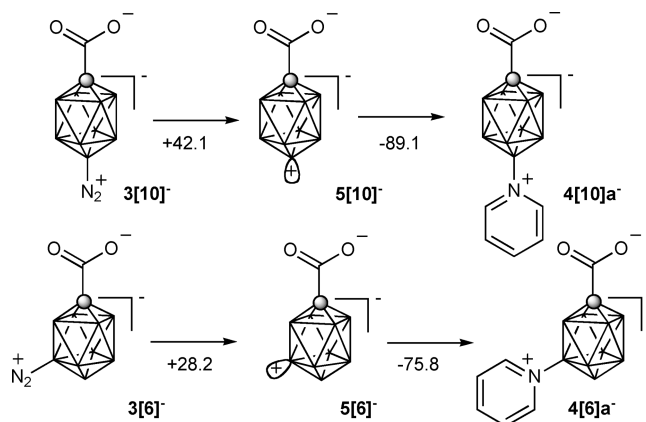


Figure 4. Enthalpy, ΔH (kcal/mol), of reaction of dinitrogen carboxylates in a pyridine dielectric medium. MP2/6-31G(d,p)//MP2/6-31G(d,p) level with density functional theory thermodynamic corrections (PCM).

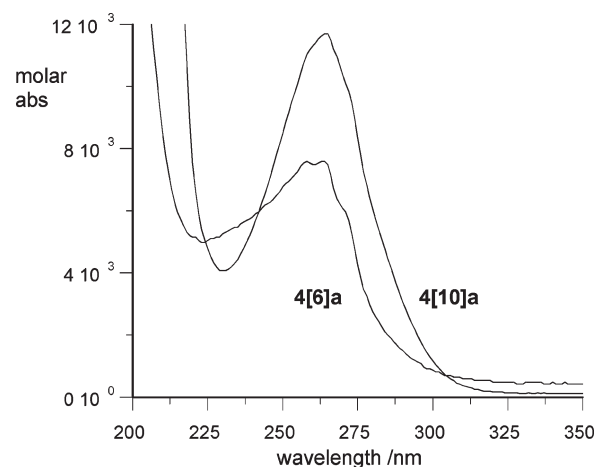


Figure 5. Electronic absorption spectra for pyridinium acids 4[6]a and 4[10]a recorded in CH_3CN .

were obtained by recrystallization from aqueous solution. Compound 4[6]d was purified only by column chromatography. Yields are calculated on the content of amino acid 1[6] in the mixture.

[*closo-1-CB₉H₈-1-COOH-6-C₅H₅N*] (**4[6]a**). Yield: 58%. $R_f = 0.3$ ($\text{CH}_3\text{OH}/\text{CH}_2\text{Cl}_2$, 1:9). Mp: $193\text{--}195^\circ\text{C}$. ^1H NMR (CD_3CN , 400 MHz): δ 0.8–2.8 (m, 8H), 5.54 (q, $J = 161 \text{ Hz}$, 1H), 7.73 (t, $J = 7.3 \text{ Hz}$, 2H), 8.26 (tt, $J_1 = 7.8 \text{ Hz}$, $J_2 = 1.4 \text{ Hz}$, 1H), 8.45 (d, $J = 5.5 \text{ Hz}$, 2H), 9.72 (s, 1H). ^{11}B NMR (CD_3CN , 128 MHz): δ -25.3 (d, $J = 152 \text{ Hz}$, 1B), -19.9 (d, $J = 154 \text{ Hz}$, 2B), -16.2 (d, $J = 165 \text{ Hz}$, 2B), -11.2 (d, $J = 157 \text{ Hz}$, 2B), -5.2 (s, 1B), 30.2 (d, $J = 160 \text{ Hz}$, 1B). UV (CH_3CN): λ_{max} (log ϵ) 264 nm (3.87). Anal. Calcd for $\text{C}_7\text{H}_{14}\text{B}_9\text{NO}_2$: C, 34.81; H, 5.84; N, 5.80. Found: C, 35.07; H, 5.84; N, 5.80.

[*closo-1-CB₉H₈-1-COOH-6-(4-CH₃O-C₅H₄N)*] (**4[6]b**). Yield: 73%. $R_f = 0.3$ ($\text{CH}_3\text{OH}/\text{CH}_2\text{Cl}_2$, 1:9). Mp: $236\text{--}238^\circ\text{C}$. ^1H NMR (CD_3CN , 400 MHz): δ 0.8–2.8 (m, 8H), 3.98 (s, 3H), 5.55 (q, $J = 159 \text{ Hz}$, 1H), 7.13 (d, $J = 6.6 \text{ Hz}$, 2H), 8.30 (d, $J = 7.4 \text{ Hz}$, 2H), 9.70 (s, 1H). ^{11}B NMR (CD_3CN , 128 MHz): δ -25.5 (d, $J = 146 \text{ Hz}$, 1B), -19.5 (d, $J = 149 \text{ Hz}$, 2B), -16.5 (d, $J = 157 \text{ Hz}$, 2B), -11.1 (d, $J = 152 \text{ Hz}$, 2B), -5.4 (s, 1B), 29.5 (d, $J = 156 \text{ Hz}$, 1B). Anal. Calcd for $\text{C}_8\text{H}_{16}\text{B}_9\text{NO}_3$: C, 35.39; H, 5.94; N, 5.16. Found: C, 35.67; H, 5.90; N, 5.04.

[*closo-1-CB₉H₈-1-COOH-6-(2-CH₃-C₅H₄N)*] (**4[6]c**). Yield: 24%. $R_f = 0.3$ ($\text{CH}_3\text{OH}/\text{CH}_2\text{Cl}_2$, 1:9). Mp: $196\text{--}198^\circ\text{C}$. ^1H NMR (CD_3CN , 400 MHz): δ 0.8–2.8 (m, 8H), 2.59 (s, 3H), 5.37 (q, $J = 157 \text{ Hz}$, 1H), 7.48 (t, $J = 6.9 \text{ Hz}$, 1H), 7.53 (d, $J = 8.0 \text{ Hz}$, 1H), 8.04 (td,

$J_1 = 7.8$ Hz, $J_2 = 1.5$ Hz, 1H), 8.11 (d, $J = 6.1$ Hz, 1H), 9.71 (s, 1H). ^{11}B NMR (CD_3CN , 128 MHz): $\delta -25.4$ (d, $J = 141$ Hz, 1B), -19.8 (d, $J = 146$ Hz, 2B), -15.6 (d, $J = 156$ Hz, 2B), -10.9 (d, $J = 157$ Hz, 2B), -5.8 (s, 1B), 30.4 (d, $J = 156$ Hz, 1B). Anal. Calcd for $\text{C}_8\text{H}_{16}\text{B}_9\text{NO}_2$: C, 37.60; H, 6.31; N, 5.48. Found: C, 37.42; H, 6.19; N, 5.32.

[*closo-1-CB₉H₈-1-COOH-6-C₉H₇N*] (**4[6]d**). Yield: 3%. $R_f = 0.3$ ($\text{CH}_3\text{OH}/\text{CH}_2\text{Cl}_2$, 1:9). ^1H NMR (CD_3CN , 400 MHz) major signals: $\delta 0.8$ – 2.8 (m, 8H), 5.46 (q, $J = 156$ Hz, 1H), 7.74 (dd, $J_1 = 8.3$ Hz, $J_2 = 5.8$ Hz, 1H), 7.83 (t, $J = 7.6$ Hz, 1H), 8.00 (td, $J_1 = 8.0$ Hz, $J_2 = 1.4$ Hz, 1H), 8.16 (d, $J = 8.0$ Hz, 1H), 8.36 (d, $J = 9.0$ Hz, 1H), 8.62 (d, $J = 5.2$ Hz, 1H), 8.79 (d, $J = 8.3$ Hz, 1H). ^{11}B NMR (CD_3CN , 128 MHz) major signals: $\delta -25.3$ (d, $J = 150$ Hz, 1B), -19.7 (d, $J = 137$ Hz, 2B), -15.3 (d, $J = 164$ Hz, 2B), -11.0 (d, $J = 156$ Hz, 2B), -5.6 (s, 1B), 31.0 (d, $J = 150$ Hz, 1B). ESI-HRMS(+). Calcd for $\text{C}_{11}\text{H}_{17}\text{B}_9\text{NO}_2$: m/z 294.2097. Found: m/z 294.2094.

Amination of a Mixture of [*closo-1-CB₉H₈-1-COOH-6-I*][−] (**2[6]**) and [*closo-1-CB₉H₈-1-COOH-10-I*][−] (**2[10]**). Following the literature procedure,⁶ a 4:1 mixture of iodo acids **2[6]** and **2[10]** (2.0 g, 5.5 mmol) was transformed into 0.370 g of product containing 74% amino acid **1[6]**, 15% amino acid **1[10]**, 7% of [*closo-1-CB₉H₈-1-COOH*][−] ([B10 (CD_3CN) δ 34.4 ppm]), and 4% of an unknown {*closo-1-CB₉*} cluster derivative ([B10 (CD_3CN) δ 40.1 ppm]), according to ^{11}B NMR. A second attempt starting from another 4:1 mixture of iodo acids **2[6]** and **2[10]** (1.34 g, 3.69 mmol) gave 0.311 g of product containing 90% amino acid **1[6]**, 7% amino acid **1[10]**, and about 3% of [*closo-1-CB₉H₈-1-COOH*][−].

Major signals attributed to [*closo-1-CB₉H₈-1-COOH-6-NH₂*] (**1[6]**). ^1H NMR (CD_3CN , 400 MHz): $\delta 0.8$ – 2.8 (m, 8H), 4.87 (t, $J = 46$ Hz, 3H), 5.6 (q, $J = 156$ Hz, 1H), 9.53 (s, 1H). ^{11}B NMR (CD_3CN , 128 MHz): $\delta -26.3$ (d, $J = 144$ Hz, 1B), -20.6 (d, $J = 144$ Hz, 2B), -16.7 (d, $J = 156$ Hz, 2B), -12.3 (s, 1B), -11.7 (d, $J = 141$ Hz, 2B), 30.0 (d, $J = 154$ Hz, 1B).

ASSOCIATED CONTENT

S Supporting Information. Table with calculated reaction energies, full crystal data collection information for **4[6]a**, archive files of MP2 equilibrium geometries for selected molecules. This material is available free of charge via the Internet at <http://pubs.acs.org>.

AUTHOR INFORMATION

Corresponding Author

*E-mail: piotr.kaszynski@vanderbilt.edu.

Notes

[‡]E-mail: bryan.ringstrand@vanderbilt.edu.

Notes

[†]E-mail: vyoung@umn.edu.

ACKNOWLEDGMENT

This project was supported by NSF Grant DMR-0907542.

REFERENCES

- Hertler, W. R.; Knoth, W. H.; Muettterties, E. L. *J. Am. Chem. Soc.* **1964**, *86*, 5434–5439.
- Hertler, W. R.; Knoth, W. H.; Muettterties, E. L. *Inorg. Chem.* **1965**, *4*, 288–293.
- Knoth, W. H. *J. Am. Chem. Soc.* **1966**, *88*, 935–939.
- Leyden, R. N.; Hawthorne, M. F. *Inorg. Chem.* **1975**, *14*, 2444–2446.

- Ringstrand, B.; Kaszynski, P.; Franken, A. *Inorg. Chem.* **2009**, *48*, 7313–7329.
- Ringstrand, B.; Kaszynski, P.; Young, V. G., Jr.; Janousek, Z. *Inorg. Chem.* **2010**, *49*, 1166–1179.
- Ng, L.-L.; Ng, B. K.; Shelly, K.; Knobler, C. B.; Hawthorne, M. F. *Inorg. Chem.* **1991**, *30*, 4278–4280.
- Naoufal, D.; Grüner, B.; Bonnetot, B.; Mongeot, H. *Polyhedron* **1999**, *18*, 931–939.
- Kaszynski, P.; Huang, J.; Jenkins, G. S.; Bairamov, K. A.; Lipiak, D. *Mol. Cryst. Liq. Cryst.* **1995**, *260*, 315–332.
- Kaszynski, P.; Douglass, A. G. *J. Organomet. Chem.* **1999**, *581*, 28–38.
- Komura, M.; Nakai, H.; Shiro, M. *J. Chem. Soc., Dalton Trans.* **1987**, 1953–1956.
- Bragin, V. I.; Sivaev, I. B.; Bregadze, V. I.; Votnova, N. A. *J. Organomet. Chem.* **2005**, *690*, 2847–2849.
- Ringstrand, B.; Kaszynski, P.; Januszko, A.; Young, V. G., Jr. *J. Mater. Chem.* **2009**, *19*, 9204–9212.
- Ringstrand, B.; Kaszynski, P. *J. Mater. Chem.* **2010**, *20*, 9613–9615.
- Ringstrand, B.; Kaszynski, P. *J. Mater. Chem.* **2011**, *21*, 90–95.
- Miniewicz, A.; Samoc, A.; Samoc, M.; Kaszynski, P. *J. Appl. Phys.* **2007**, *102*, 033108.
- Kaszynski, P.; Pakhomov, S.; Young, V. G., Jr. *Collect. Czech. Chem. Commun.* **2002**, *67*, 1061–1083.
- Ringstrand, B.; Balinski, A.; Franken, A.; Kaszynski, P. *Inorg. Chem.* **2005**, *44*, 9561–9566.
- The yield and proportions of the two amino acids vary from run to run presumably because of the quality of $\text{LiN}(\text{TMS})_2$ and the workup details.
- Gero, A.; Markham, J. J. *J. Org. Chem.* **1951**, *16*, 1835–1838.
- Murmann, R. K.; Basolo, F. *J. Am. Chem. Soc.* **1955**, *77*, 3484–3486.
- Albert, A.; Goldacre, R.; Phillips, J. *J. Chem. Soc.* **1948**, 2240–2249.
- Crystal data for **4[6]a** (CCDC no. 804225): $\text{C}_2\text{H}_9\text{B}_9\text{NO}_2$, monoclinic, $P2_1/n$, $a = 6.6504(7)$ Å, $b = 18.4803(18)$ Å, $c = 10.8552(11)$ Å, $\beta = 96.833(1)^\circ$, $V = 1324.6(2)$ Å³, $Z = 4$, $T = 123(2)$ K, $\lambda = 0.71073$ Å, $R(F^2) = 0.0387$ or $R_w(F^2) = 0.0999$ [for 2252 reflections with $I > 2\sigma(I)$]. For details, see the Supporting Information.
- Jelinek, T.; Plešek, J.; Hermanek, S.; Stibr, B. *Collect. Czech. Chem. Commun.* **1986**, *51*, 819–829.
- For details, see the Supporting Information.
- Swain, C. G.; Sheats, J. E.; Harbison, K. G. *J. Am. Chem. Soc.* **1975**, *97*, 783–790.
- The calculated excitation energy depends on the radius of the cavity used in the SCRF calculations. For the two acids, higher energies are obtained for smaller cavities.
- Low yields of *N*-pyridine derivatives of $[\text{B}_{12}\text{H}_{12}]^{2-}$ were obtained using a different method. Vöge, A.; Lork, E.; Sesalan, B. S.; Gabel, D. *J. Organomet. Chem.* **2009**, *694*, 1698–1703. Koch, T.; Preetz, W. *Z. Naturforsch.* **1997**, *52B*, 939–942 and 1165–1168.
- Becke, A. D. *J. Chem. Phys.* **1993**, *98*, 5648–5652.
- Lee, C.; Yang, W.; Parr, R. G. *Phys. Rev. B* **1988**, *37*, 785–789.
- Møller, C.; Plesset, M. S. *Phys. Rev.* **1934**, *46*, 618–622. Head-Gordon, M.; Pople, J. A.; Frisch, M. J. *Chem. Phys. Lett.* **1988**, *153*, 503–506.
- Frisch, M. J. et al. *Gaussian 09*, revision A.02; Gaussian, Inc.: Wallingford, CT, 2009.
- Scott, A. P.; Radom, L. *J. Phys. Chem.* **1996**, *100*, 16502–16513.
- Foresman, J. B.; Keith, T. A.; Wiberg, K. B.; Snoonian, J.; Frisch, M. J. *J. Phys. Chem.* **1996**, *100*, 16098–16104.
- Hasted, J. B. In *Water a Comprehensive Treatise*; Franks, F., Ed.; Plenum Press: New York, 1973; Vol. 2, p 421.
- Zerner, M. C. In *Reviews of Computational Chemistry*; Lipkowitz, K. B., Boyd, D. B., Eds.; VCH Publishing: New York, 1991; Vol. 2, pp 313–366 and references cited therein.